

---

# PROGRESSIVE ENERGY-BASED COOPERATIVE LEARNING FOR MULTI-DOMAIN IMAGE-TO-IMAGE TRANSLATION

---

Weinan Song<sup>1</sup>, Yaxuan Zhu<sup>1</sup>, Lei He<sup>2,1</sup>, Yingnian Wu<sup>1</sup>, and Jianwen Xie<sup>3</sup>

<sup>1</sup>University of California, Los Angeles

<sup>2</sup>Eastern Institute for Advanced Study, Ningbo, China

<sup>3</sup>Akool Research

## ABSTRACT

This paper studies a novel energy-based cooperative learning framework for multi-domain image-to-image translation. The framework consists of four components: descriptor, translator, style encoder, and style generator. The descriptor is a multi-head energy-based model that represents a multi-domain image distribution. The components of translator, style encoder, and style generator constitute a diversified image generator. Specifically, given an input image from a source domain, the translator turns it into a stylised output image of the target domain according to a style code, which can be inferred by the style encoder from a reference image or produced by the style generator from a random noise. Since the style generator is represented as an domain-specific distribution of style codes, the translator can provide a one-to-many transformation (i.e., diversified generation) between source domain and target domain. To train our framework, we propose a likelihood-based multi-domain cooperative learning algorithm to jointly train the multi-domain descriptor and the diversified image generator (including translator, style encoder, and style generator modules) via multi-domain MCMC teaching, in which the descriptor guides the diversified image generator to shift its probability density toward the data distribution, while the diversified image generator uses its randomly translated images to initialize the descriptor’s Langevin dynamics process for efficient sampling. We also bring in two regularization strategies for both the descriptor and the translator to significantly improve the cooperative learning. To further enhance the efficiency and scalability, we propose a progressive cooperative learning strategy to train our framework from low resolution to high resolution. Strong empirical results on CelebA-HA and AFHQ datasets are shown to verify the effectiveness of our energy-based image translation framework.

## 1 Introduction

The task of image-to-image translation primarily involves the learning of mappings between different visual domains. This learning framework carries immense application value in the field of generative artificial intelligence, facilitating the development of various creative products for artificial intelligence-generated contents (AIGC). In this context, a “domain” refers to a collection of images belonging to a visually distinctive category such as the gender of a person and animal species. Within each domain, every image exhibits a unique appearance, encompassing image-specific elements such as hairstyle and makeup, commonly referred to as its “style”. An ideal image-to-image translation framework should possess the ability to handle multiple domains, efficiently process high-resolution images, and provide diverse synthesis (i.e., one-to-many mapping) when translating to each target

domain. While several pioneering work [1, 2] have made significant strides towards this goal, it is noteworthy that they predominantly rely on adversarial learning techniques. In contrast, our paper explores the multi-domain image-to-image translation problem using energy-based modeling techniques. This research is motivated by the current swift advancements in energy-based modeling and learning technologies.

By leveraging the representation power of an energy-based model and the sampling efficiency of a latent variable model, the Generative Cooperative Network [3], also known as CoopNets, and its variants [4, 5], have achieved impressive results in numerous computer vision tasks, such as image generation [3, 4, 5], visual salient object detection [6], supervised image-to-image translation [7], and unsupervised image-to-image translation [8]. However, while the cross-domain translation framework, CycleCoopNets [8], has demonstrated success in unpaired image-to-image translation, it is only capable of learning the relation between two different domains at a time. Such an approach has a limited scalability in deal with multiple domains, as a separate model must be trained for each pair of domains. In addition, cooperative learning still faces challenges when it comes to translating high-resolution images. This is because the translation process involves sampling from the energy-based model via Langevin dynamics, which can be difficult to apply to high-resolution image spaces. To tackle the aforementioned challenges existing in the current cooperative learning (or more generally, energy-based learning) for multi-domain unsupervised image-to-image translation, this paper proposes a novel cooperative learning framework, MD-CoopNets, to ensure **scalability**, **flexibility**, **stability** and **efficiency** for applying energy-based framework to image-to-image translation.

To be specific, the MD-CoopNets consists of four components: descriptor, translator, style generator and style encoder. (1) The descriptor is a multi-head energy-based model that represents a multi-domain image distribution, where each head of the energy function corresponds to one image domain. (2) The style generator is a multi-head latent variable model responsible for generating domain-specific style codes. It achieves this by transforming a Gaussian latent code into a style code. Each head in the style generator corresponds to one specific domain. It represents a domain-specific distribution of style codes. (3) The style encoder extracts domain-specific style codes from an input image using a multi-head encoder. Each head of the encoder corresponds to a specific domain. (4) The translator is a style-controlled mapping, which takes an image and a style code as input, and then transforms the image into a translated image that reflects the desired style indicated by the style code. The style code can be obtained either from the style generator or the style extractor. The style generator, style encoder, and style-controlled translator can constitute a diversified image generator.

As to the learning, the multi-domain descriptor and the diversified image generator engage in a cooperative game, where the multi-domain descriptor guides the diversified image generator in aligning its mapping towards the target domains using MCMC teaching, while the image generator assists in expediting the descriptor’s MCMC teaching process by providing a good initialization. Specifically, to enforce a meaningful latent space of style codes, we train the style-controlled translator and style encoder by reconstructing style codes that are randomly generated from the style generator. To enforce translated image to preserve the domain-invariant property of the input reference image, we train the translator with a cycle consistency loss. To enforce the one-to-many translation output, we regularize the translator via a diversity sensitive loss, such that, given an identical reference image, different style codes can lead to sufficiently diversified translated outputs.

Additionally, we propose to improve the cooperative learning algorithm by incorporating some loss terms to regularize the behaviors of the components in our framework. Firstly, we put an  $l_2$  regularization on the output of the energy function of the descriptor to limit the magnitude of the energy values. To accelerate and stabilize the teaching process provided by the descriptor’s MCMC, we propose to use the energy function to regularize the output of the translator. These regularization techniques significantly improve the performance of the cooperative learning.

To enhance efficiency, stability, and scalability, we present a novel progressive cooperative learning algorithm for our model. Our approach involves a gradual expansion of the components, initially operating on simpler low-resolution images. As the cooperative training proceeds, new layers are added to each component, enabling the model to handle more challenging high-resolution images. This progressive growth strategy significantly accelerates and stabilizes both training and sampling processes at higher resolutions. Moreover, it offers the flexibility and convenience to scale up the resolution of any pre-trained MD-CoopNets.

We demonstrate the effectiveness of our proposed multi-domain translation model on the CelebA-HQ [9] and AFHQ [2] dataset. The translated examples exhibit high fidelity and are comparable to GAN-based multi-domain translation models. Furthermore, our progressive learning strategy improves the efficiency and stability of the original training process, particularly when it comes to translating high-resolution images.

Our contributions are listed as follows:

- We propose a novel energy-based cooperative learning framework for multi-domain image-to-image translation. We build a single multi-head energy-based model to represent probability distributions of multiple domains, and train it with a translator, a style encoder, and a style generator using a cooperative manner.
- We present a novel progressive learning algorithm to optimize the training efficiency of our framework. Our approach adopts a progressive growth strategy, advancing all components from low resolution to high resolution. It yields a significant reduction in the total number of MCMC steps required for training and sampling from the high-resolution model.
- We propose regularization strategies to stabilize the cooperative learning, which include an energy-based regularization loss for the translator and a  $l_2$  regularization loss for limiting the magnitude of the energy values of the descriptor. Significant performance gain are obtained from these regularization.
- We demonstrate strong empirical results on CelebA-HQ and AFHQ datasets to verify the proposed energy-based framework. Our method obtains state-of-the-art performance among existing energy-based image translation models and comparable results with GAN-based baselines.

## 2 Related Work

**Energy-based Learning** Training energy-based models (EBMs) [10, 11, 12] involves maximizing the likelihood of the observed data by adjusting the model’s energy function parameters, which typically requires Markov chain Monte Carlo (MCMC) sampling to evaluate the intractable gradient [13, 14, 15]. Contrastive divergence (CD) [16, 17] is an efficient approximation algorithm for training energy-based models by initializing the MCMC chains with observed data. [14] uses a noise-initialized non-convergent short-run MCMC to train an EBM, and obtains a valid flow-like generator trained with moment matching estimation. [18] defines a sequence of conditional EBMs and forms a denoising diffusion process. To avoid MCMC, [19] brings in normalizing flow and trains an EBM by flow contrastive estimation. Learning an amortized sampler [20, 3, 21, 22, 23, 24] for EBMs is also an alternative strategy. Our method has a single multi-head EBM to represent multi-domain data distribution, and the image-to-image translator serves as a multi-domain amortized sampler for the EBMs.

**Cooperative Learning** Cooperative learning for energy-based models with MCMC teaching is first proposed in [3], where the authors utilize an energy-based model as the descriptor and a latent variable model as the generator to speed up the learning of each other by maximum likelihood algorithms. During each training iteration, the descriptor generates samples by finite-step MCMC sampling with initialization by the generation from the generator for maximum likelihood estimation. Simultaneously, the sampling results from descriptor are used to directly supervise the generator, which is called MCMC teaching. Further research in [25] shows that this cooperative learning method could also provide a good start point for adversarial models with small computation overhead. Additionally, the model could also be extended for image-to-image translation [8] with two pairs of descriptor and generator or used in saliency prediction [26] by introducing a conditional latent variable model.

**Progressive Learning** The proposed idea of progressive cooperative learning is closely connected to the research conducted by [27], which involves the incremental growth of a single EBM. The multi-grid EBM framework [28], trains a series of EBMs simultaneously at various resolutions. The sampling process is conducted sequentially, starting from low-resolution and gradually progressing to higher resolutions, leveraging the lower resolution as a foundation for subsequent higher-resolution sampling. In contrast, our method, which combines the growth of an EBM with three mapping

networks, introduces a more challenging and complex progressive learning strategy. It is important to note that while there are several progressive learning frameworks based on Generative Adversarial Networks (GANs), our approach falls within the domain of energy-based learning. We need to carefully consider MCMC sampling when progressively expanding the energy function, as it plays a crucial role in both the bottom-up energy mapping and top-down image generation.

### 3 Proposed Framework

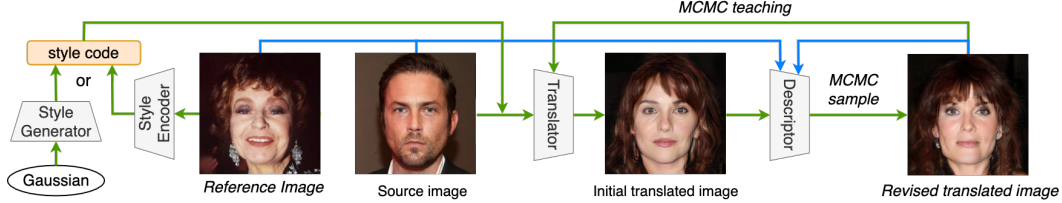


Figure 1: Diagram of cooperative learning for multi-domain image-to-image translation. The framework consists of a style generator, a style encoder, a translator and a descriptor. Given an input source image, the translator can transform it into a target domain, which is specified by a style code. The style code can be obtained by sampling from the domain-specific style generator or extracted from a reference image by the style encoder. The descriptor is a multi-domain image distribution, which plays the role of guiding the translation such that the translated images can match the observed images in the target domain in terms of statistical property. All components are trained simultaneously in a cooperative learning scheme. The descriptor learns from the multi-domain training images by maximizing the data likelihood, while utilizing MCMC teaching to guide the training of the translator, style encoder, and style generator.

Suppose we have unpaired images from multiple domains  $A, B, C, \dots$  with some shared high-level features, such as expressions in face images, our target is to learn a conditional generative model that maps an image into a target domain, which could be same as the source domain, with specific features. To achieve this, we propose a generative model that consists of four components, i.e., descriptor, style encoder, style generator, and translator. The latter three can form a diversified translator, which is trained with the descriptor in a cooperative learning manner. Let  $x$  be an observed image and  $y$  be its domain label. We also use  $y'$  to denote the label of target domain.

#### 3.1 Multi-Domain Image Descriptor

The multi-domain image descriptor is a multi-head energy-based model that specifies the probability distribution of each domain by

$$p_y(x; \theta) \propto \exp[D_y(x; \theta)], \quad (1)$$

where  $\theta$  are parameters of the multi-head energy function  $D$ . For notation simplicity, we use  $D_y(\cdot)$  to denote the negative energy for domain  $y$ . The descriptor are learned by multi-domain maximum likelihood estimation, which is equivalent to minimizing the Kullback-Leibler (KL) divergence between the data distribution  $p_{\text{data}}(x, y)$  and the model  $p_y(x; \theta)$ . The gradient of the objective for learning the descriptor is given by

$$\nabla_{\theta} \mathcal{L}_{\text{ebm}}(\theta) = -\mathbb{E}_{p_{\text{data}}(x, y)} \{ \nabla_{\theta} D_y(x; \theta) - \mathbb{E}_{p_y(x'; \theta)} [\nabla_{\theta} D_y(x'; \theta)] \}, \quad (2)$$

where  $\mathbb{E}_{p_y(x'; \theta)}$  denotes the expectation with respect to the EBM and we use  $x'$  in order to distinguish the random variable  $x$  in  $\mathbb{E}_{p_{\text{data}}(x, y)}$  in the same equation. Suppose we observe a batch of training examples  $\{(x_i, y_i)\}_i^n$ , which is assumed to be from  $p_{\text{data}}(x, y)$ . The gradient in Eq.(2) can be approximated by

$$\nabla_{\theta} \mathcal{L}_{\text{ebm}}(\theta) \approx \nabla_{\theta} \left[ \frac{1}{n} \sum_{i=1}^n D_{y_i}(x_i; \theta) - \frac{1}{n} \sum_{i=1}^n D_{y_i}(\tilde{x}_i; \theta) \right], \quad (3)$$



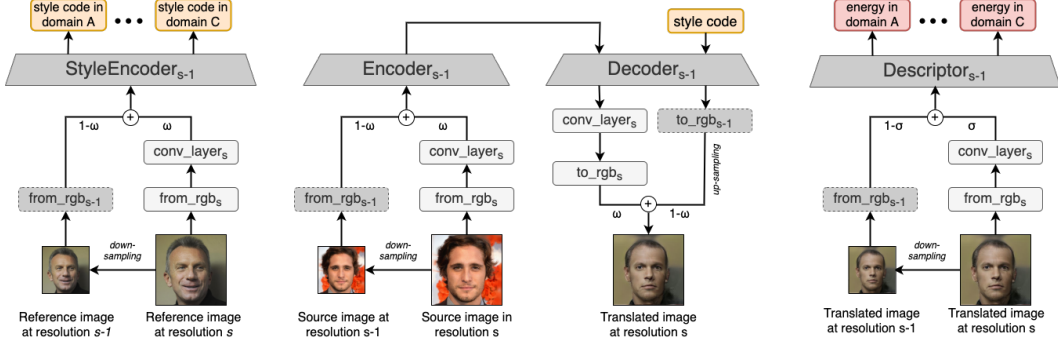


Figure 2: An illustration of the progressive strategy for the style encoder  $E$ , translator  $T$ , and descriptor  $D$ . Boxes in dark grey represent well-trained modules at resolution level  $s - 1$ , while blocks in light grey represent the newly added parameters at the current resolution level  $s$ . The expansion of the model involves removing some incompatible parameters (depicted as dark grey boxes with dashed boundaries) and adding new parameters (depicted as light grey boxes). The output of the module that needs to be removed and the output of the module that needs to be added are fused using a transition factor  $\omega$ . This factor starts from 0 and gradually increases to 1, controlling the percentage of contribution from the old and new modules. Left: style encoder. Middle: style-controlled image-to-image translator. Right: descriptor.

where for each observed domain  $y_i$ , we use Langevin dynamics to obtain the corresponding synthesized example  $\tilde{x}_i$  as a sample from  $p_{y_i}(x; \theta)$ . With a specified step size  $\delta$ , Langevin dynamics is performed by iterating the follow step

$$\tilde{x}_{\tau+1} = \tilde{x}_{\tau} + \delta \nabla_x D_y(\tilde{x}_{\tau}; \theta) + \sqrt{2\delta} U_{\tau}, \quad U_{\tau} \sim \mathcal{N}(0, I), \quad (4)$$

where  $\tau$  indexes time step and  $\tilde{x}_{\tau=0}$  is initialized by the output of a style-controlled image-to-image translator, which is presented in Section 3.2. A good initialization improves the efficiency of Langevin dynamics. To stabilize the EBM training, we also add an  $l_2$  regularization on the energy outputs of both training examples and synthesized examples, which is

$$\mathcal{L}_{\text{energy}}(\theta) = \frac{1}{n} \sum_{i=1}^n \|D_{y_i}(x_i; \theta)\|^2 + \frac{1}{n} \sum_{i=1}^n \|D_{y_i}(\tilde{x}_i; \theta)\|^2. \quad (5)$$

### 3.2 Diversified Image Generator

**Multi-Domain Style Generator** Given a latent variables  $z$  and a domain label  $y$ , the multi-domain style generator can produce a domain-specific style code  $c$  by

$$c_y = G_y(z; \beta) + \epsilon, \quad \epsilon \sim \mathcal{N}(0, I), z \sim \mathcal{N}(0, I), \quad (6)$$

where  $\epsilon$  is an observation residual and  $z$  follows a Gaussian prior distribution.  $G$  is a multilayer perceptron (MLP) with multiple output branches to produce style codes for multiple domains. The distribution of style code  $c$  conditioned on a domain  $y$  is given by  $p_y(c; \beta) = \int p_y(c|z; \beta)p(z)dz$ , which is more informative than the prior distribution  $p(z)$  to capture the underlying style space. The domain-specific style code  $c_y$  is directly used in the translator, which is presented in Section 3.2, for specifying the style and the target domain of the translated image.

**Style Encoder** The style encoder  $E$  is a multi-head bottom-up network that takes as input an image  $x$  and its corresponding domain label  $y$  and then outputs a domain-specific style code  $c = E_y(x; \phi)$ , where  $\phi$  are parameters and  $E_y(\cdot)$  denotes the output of  $E$  that corresponds to domain  $y$ .

**Style-Controlled Image-to-Image Translator** To achieve a one-to-many translation between domains, we build a style-controlled image-to-image translator. It is a conditioned encoder-decoder

$T$  that takes as input a source reference image  $x$  and a domain-specific style code  $c_y$  and outputs a translated image in target domain  $y$ , which is given by

$$x_y = T(x, c_y; \alpha) + \epsilon, \quad \epsilon \sim \mathcal{N}(0, I), c_y \sim p_y(c; \beta), \quad (7)$$

where  $\alpha$  is the parameters of the neural network  $T$ . The randomness in the translated image, when given a reference image and the target domain, arises from the stochastic nature of the style codes, which follows a distribution defined by the style generator  $p_y(c; \beta)$ . The translator  $T$  and the style generator  $G$  forms a diversified translator. They are trained by the MCMC teaching loss:

$$\mathcal{L}_{\text{teach}}(\alpha, \beta) = \mathbb{E}_{z,y,x} [\|\tilde{x}_{z,y,x} - T(x, G_y(z; \beta); \alpha)\|^2], \quad (8)$$

where  $\tilde{x}_{z,y,x}$  denotes the Langevin synthesis from the descriptor, which is initialized by the output of  $T(x, G_y(z; \beta); \alpha)$ . That is, we set  $\tilde{x}_{z,x,y,\tau=0} \leftarrow T(x, G_y(z; \beta))$  for Langevin dynamics in Eq.(4) to revolve  $\tilde{x}_{z,y,x}$ . Let  $M_\theta q_{\alpha,\beta}(x)$  be the marginal distribution obtained by running Markov transition  $M_\theta$  from  $q(x; \alpha, \beta)$ . At learning step  $t + 1$ , the gradient of the MCMC teaching loss in Eq.(8) is the gradient of  $\text{KL}(M_{\theta(t)} q_{\alpha(t), \beta(t)} \| q_{\alpha, \beta})$ , where  $q_{\alpha, \beta}$  seeks to be the stationary distribution of  $M_\theta$ , i.e., minimizing  $\text{KL}(p_\theta \| q_{\alpha, \beta})$ . The effects of the MCMC teaching loss include: (i)  $q$  can chase  $p$  toward  $p_{\text{data}}$  for MLE; (ii)  $q$  can serve as a good MCMC initializer for  $p$  for efficient MCMC sampling. To ensure diverse translator outputs, we regularize  $T$  by minimizing the negative diversity sensitive

$$\mathcal{L}_{\text{diverse}}(\alpha) = -\mathbb{E}_{z_1, z_2, y, x} [\|T(x, G_y(z_1; \beta); \alpha) - T(x, G_y(z_2; \beta); \alpha)\|_1]. \quad (9)$$

Since the translator is learned from unpaired data domains, to ensure the translated image  $T(x, c; \alpha)$  to preserve the domain-invariant features of the source image  $x$ , we adopt the cycle consistency loss

$$\mathcal{L}_{\text{cycle}}(\alpha) = \mathbb{E}_{z,y,x,y'} [\|x - T(T(x, G_{y'}(z; \beta); \alpha), E_y(x; \phi); \alpha)\|_1]. \quad (10)$$

To ensure any style code that is applied to the translated image can be retrieved back from the translated image by the style encoder, we also have a style code reconstruction loss

$$\mathcal{L}_{\text{style}}(\alpha, \phi) = \mathbb{E}_{z,y',x} [\|G_{y'}(z; \beta) - E_{y'}(T(x, G_{y'}(z; \beta); \alpha); \phi)\|_1]. \quad (11)$$

To further stabilize the cooperative training and accelerate the MCMC teaching effect, we propose to add the following energy-based regularization on the translator,

$$\mathcal{L}_{\text{mode}}(\alpha, \beta) = \mathbb{E}_{z,y',x} [D_{y'}(T(x, G_{y'}(z; \beta); \alpha); \theta)], \quad (12)$$

which can shift the translator mapping toward the low energy modes of the energy function.

### 3.3 Cooperative Learning of Image Descriptor and Image Generator

Our full objective function of the image descriptor is  $\mathcal{L}_{\text{descriptor}} = \mathcal{L}_{\text{ebm}} + \lambda_{\text{energy}} \mathcal{L}_{\text{energy}}$  and the full objective function of the image generator is  $\mathcal{L}_{\text{generator}} = \mathcal{L}_{\text{teach}} + \lambda_{\text{diverse}} \mathcal{L}_{\text{diverse}} + \lambda_{\text{cycle}} \mathcal{L}_{\text{cycle}} + \lambda_{\text{style}} \mathcal{L}_{\text{style}} + \lambda_{\text{mode}} \mathcal{L}_{\text{mode}}$ , where  $\lambda_{\text{energy}}$ ,  $\lambda_{\text{diverse}}$ ,  $\lambda_{\text{cycle}}$ ,  $\lambda_{\text{style}}$ , and  $\lambda_{\text{mode}}$  are hyperparameters. At each learning iteration, the cooperative learning algorithm alternates the following steps: (1) Generate an initial translated image via  $\hat{x} = T(x, G_y(z))$ ; (2) Revise  $\hat{x}$  by Langevin dynamics in Eq.4 to obtain  $\tilde{x}$ ; (3) Update the parameters  $\theta$  of descriptor by minimizing  $\mathcal{L}_{\text{descriptor}}$ ; (4) Update the parameters  $\alpha, \phi, \beta$  of generator by minimizing  $\mathcal{L}_{\text{generator}}$ .

### 3.4 Progressive Cooperative Learning

The update of both descriptor and generator relies on the cooperative generation of MCMC synthesized examples, denoted as  $\tilde{x}$ . To significantly improve training efficiency, we propose a progressive learning strategy for our cooperative learning framework. The algorithm gradually enhances the model resolution from low to high, while maintaining cooperative learning across all components at each resolution. The underlying motivation behind this strategy is that learning and sampling from a low resolution data domain is much more efficient. By leveraging a pre-trained low resolution model as a foundation, we can efficiently learn the next scale of the model, rather than starting from scratch. When expanding the current model to the next scale, each component's network structure undergoes modifications. New layers are added to handle higher resolution image inputs or outputs, while incompatible old layers are removed. The newly added layers are trained together with the remaining parameters. To ensure a smooth transition and prevent gradient exposure due to the addition of

expanding blocks in each component, we propose to retain partial effects of the parameters that need to be removed while incorporating the effects of the newly added parameters. Throughout each resolution of learning, the impact of the removed parameters gradually diminishes until it becomes zero. Figure 2 illustrates the expanding strategy of each component at every level of resolution. Here,  $\omega$  represents a transition factor that starts from 0 and increase to 1, controlling the percentage of effects from the parameters to be removed (depicted as dark grey boxes with dashed boundaries) and the parameters to be added (depicted as light grey boxes). For a complete description of the proposed progressive cooperative learning algorithm, please refer to Algorithm 1.

## 4 Experiment

### 4.1 Experiment Settings

**Dataset and evaluation metrics** To demonstrate the performance of our proposed multi-domain image-to-image translation framework, we test it on the CelebA-HQ [9] and AFHQ [2] datasets and compare it with several baselines. We use M and F to refer the domains of male and female in CelebA-HQ, and C, D and W to refer to the domains of cat, dog, and wild animals in AFHQ. We only use the images and the corresponding domain labels from the datasets in our experiments. We evaluate the quality of translated images using the Fréchet inception distance (FID) [29], which is a metric to measure the distance between the population of translated images and the population of original images in the target domain. A small FID is desired to indicate that the translated distribution is very close to the target distribution.

#### Hyper-parameters and network architectures

We use bottom-up convolutional neural networks to parameterize the descriptor and style encoder and use a 8-layer multilayer perceptron (MLP) for the style generator. The Translator utilizes an encoder-decoder architecture with AdaIN [30] for style control in the decoding part. As to the progressive learning, we start from training our model with a resolution of  $64 \times 64$ , and then gradually expand the model to resolutions of  $128 \times 128$  and  $256 \times 256$  in sequence. We employ 16 Langevin steps for MCMC sampling at the initial stage of the algorithm, and then reduce the number of steps by 4 after each stage of expansion. The hyperparameters of  $\lambda_{\text{energy}}$ ,  $\lambda_{\text{diverse}}$ ,  $\lambda_{\text{cycle}}$ ,  $\lambda_{\text{style}}$ , and  $\lambda_{\text{mode}}$  are set to be 1. We show the details of the network structures in Figure 3, in which the modules depicted with dotted lines indicate that they will be omitted during model expansion. Since the style generator does not involve changes in image resolution, its architecture remains unchanged as progressive learning progresses. For each DownBlock/UpBlock module at each expansion stage  $s$ , the input and output channels are set to  $\max(512, 2^{5+s})$  and  $\max(512, 2^{6+s})$ , respectively. In the fully-connected (FC) Layer of the style generator, the input channel of the top FC Layer is set to 16, while the remaining FC Layers have an input channel of 512. The size of the style code is consistently set to 64 for all experiments.

---

#### Algorithm 1 Progressive Cooperative Learning

---

**Input:** Multi-resolution data  $\{(x_i^{(s)}, y_i^{(s)}), i = 1, \dots, N; s = 1, \dots, S\}$   
**Output:** Model  $E^{(S)}, T^{(S)}, D^{(S)}, G$

```

 $E^{(0)} \leftarrow \emptyset, D^{(0)} \leftarrow \emptyset, T^{(0)} \leftarrow \emptyset$ 
for  $s = 1, \dots, S$  do
   $m \leftarrow 0$ 
  if  $s == 1$  then
     $\omega \leftarrow 1$ 
  else
     $\omega \leftarrow 0$ 
  end if
   $E^{(s, \omega)} \leftarrow \text{expand}(E^{(s-1)})$ 
   $D^{(s, \omega)} \leftarrow \text{expand}(D^{(s-1)})$ 
   $T^{(s, \omega)} \leftarrow \text{expand}(T^{(s-1)})$ 
  while  $(m \leq N)$  do
    Sample  $(x, y)$  and  $y'$ 
    Sample  $z \sim \mathcal{N}(0, I)$ 
     $c \leftarrow E_y^{(s, \omega)}(x)$  or  $c \leftarrow G_{y'}(z)$ 
     $\hat{x} \leftarrow T^{(s, \omega)}(x, c)$ 
    Revise  $\hat{x}$  to obtain  $\tilde{x}$  by a  $K$ -step Langevin dynamics in Eq. (4).
    Update descriptor  $D^{(s, \omega)}$  with  $\mathcal{L}_{\text{descriptor}}$ 
    Update translator  $\{E^{(s, \omega)}, T^{(s, \omega)}, G\}$  with  $\mathcal{L}_{\text{translator}}$ 
     $m \leftarrow m + n^{(s)}$ 
    if  $s \neq 1$  then
       $\omega \leftarrow \min(1, m/N)$ 
    end if
  end while
end for

```

---

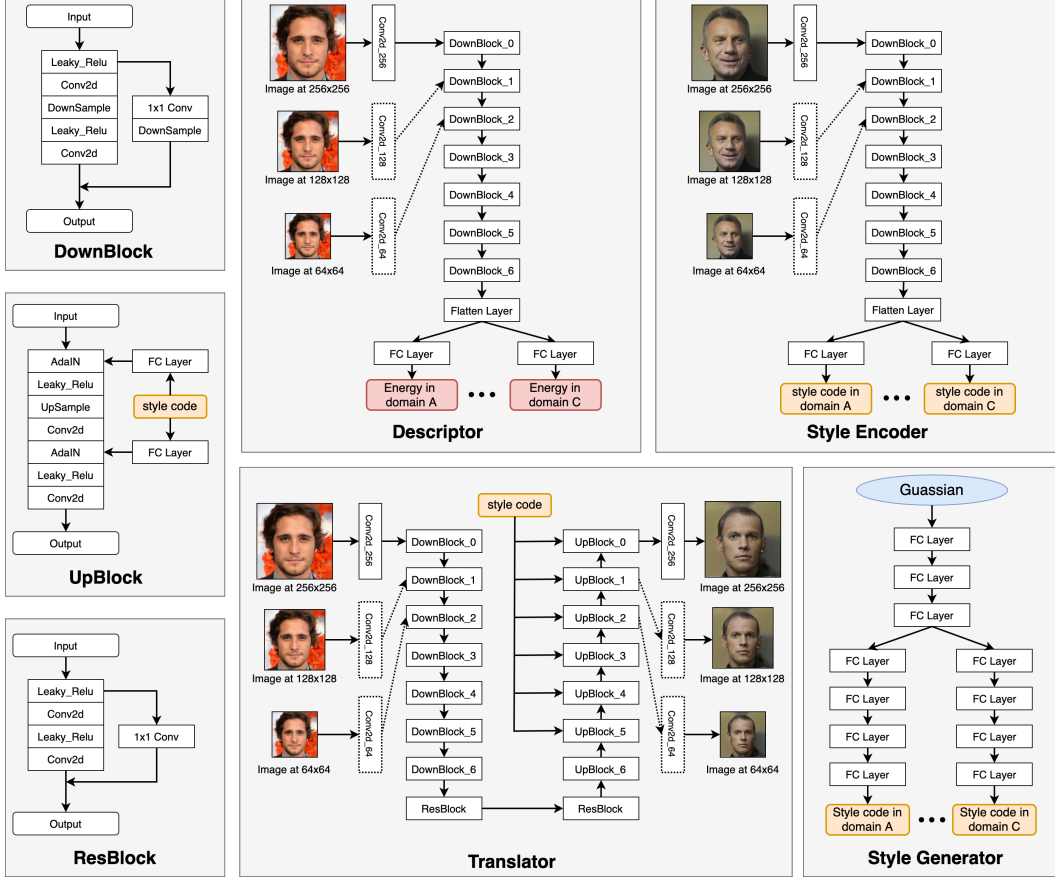


Figure 3: Illustration of network architectures for the descriptor, translator, style Generator, and style Encoder in the proposed progressive cooperative learning framework for multi-domain image-to-image translation. The modules depicted with dotted lines indicate that they will be omitted during model expansion.

## 4.2 Diverse Image Generation

In this experiment, we use style codes that are randomly sampled from the style generator to generate diverse translated images. Examples of generation results on the CelebA-HQ dataset can be seen in Figure 4. For each source image shown in the first row, we generate multiple outputs using random Gaussian noise. The qualitative results verify the diversity of the translated results from a source input image. We observe that, given a source image, our model can not only generate diverse translated images but also produce high-quality images that obtain the same attribute (e.g., expression) from the source image. Figure 5 exhibits qualitative results for the AFHQ dataset. It is evident that our model successfully produces diverse, reasonable, and realistic translated images.

## 4.3 Image-to-Image Translation using reference image

In our image-to-image translation approach, we can incorporate a reference image. To begin with, we adopt the style encoder to extract the style code from the provided reference image. Subsequently, we apply the style code to the translator network, enabling the generation of translated images based on the desired style conveyed by the reference image. Figure 6 show some qualitative results obtained on dataset CelebA-HQ, where we take images in the first row as source images and images in the first column as reference images. The translation results are shown in the middle. Comparing results displayed in each row, we can observe that the human face in the source image can be clearly changed into the same gender and appearance of the face in the reference image, while keeping the facial



Figure 4: Qualitative results of diverse image generation on CelebA-HQ dataset. Each column displays one example of one-to-many image generation. The first row displays source images. The rest four rows show different translated images, which are obtained by using four style codes randomly generated by the style generator. The style generator produces style codes by randomly sampling from Gaussian distribution.

expression consistent with that in the source domain. Figure 7 presents examples demonstrating the usage of reference images for image-to-image translation in the AFHQ dataset. These results align with our observations and findings. The translated images exhibit similar appearance styles as the reference image, indicating that they successfully capture the desired target domain properties. Simultaneously, the translated images preserve the geometry aspects, including shapes and poses, from the source images. This indicates that our approach effectively maintains the essential characteristics of the source images while incorporating the desired style from the reference image.

To verify the cycle consistency of our model, we conduct experiments for cycle image-to-image translation. Firstly, we perform an image-to-image translation from the source domain to the target domain, guided by a reference image. Then, we reverse the translation by taking the translated image as the new source image and translating it back to the original domain. We assess the quality of the cycle consistency through qualitative results, displayed in Figure 8 for the CelebA-HQ dataset and Figure 9 for the AFHQ dataset. The qualitative results clearly demonstrate that our model exhibits excellent cycle consistency properties. It effectively preserves the geometric features of the source image while applying the appearance properties from the reference image during translation in both directions. By comparing the images in the first and fourth rows, we can see that our algorithm can maintain a high level of synthesis quality and provide reasonable results in a sequential usage of the model. Our model can ensure a high level of fidelity and consistency in the translation process.

We also illustrate the progressive learning process by showcasing translated images at various resolutions. Figure 10 presents the results for the CelebA-HQ dataset, while Figure 11 showcases the results for the AFHQ dataset. Each column in the figures corresponds to translated images generated by models at different stages of resolution, using a specific source image and reference image. As observed, the generated images become more detailed as the model resolution increases.

#### 4.4 Quantitative Comparison

We also compare the results of our translation results quantitatively by using style codes from Style Encoder by randomly selecting reference image in different domains or from Style Generator through sampling from Gaussian distribution. For each source image in the validation dataset, we obtain ten translated images for each target domain to compute the FID. Results are shown in Table 1 for CelebA-HQ and Table 2& 3 for AFHQ. We compare our model with other baselines, including GAN-based method, StarGAN v2 [2], and energy-based method, CycleCoop [8]. We could see that our model could significantly outperform existing cooperative learning methods with additional ability of guidance by reference images and reach comparable performance with GAN-based methods.





Figure 5: Qualitative results of diverse image generation on AFHQ dataset. Each column show one example of one-to-many image generation. The first row displays source images and the rest six rows show different translated images generated by using different style codes sampled from the style generator.



Figure 6: We show the translated images with style codes generated from the Style Encoder and reference images in CelebA-HQ dataset in this picture. The source images and reference images are put in the first row and first column. We could see that the face has successfully translated into target domains with consistency in expression.

#### 4.5 Ablation Study

We conduct an ablation study to evaluate the importance of each individual component proposed in our paper. In Table 4, we report the model performance in terms of FID by removing different key loss term (including  $\mathcal{L}_{\text{diverse}}$ ,  $\mathcal{L}_{\text{cycle}}$ ,  $\mathcal{L}_{\text{energy}}$ ,  $\mathcal{L}_{\text{mode}}$ ) from our objective function in our framework. We train our model in a  $64 \times 64$  resolution setting on datasets CelebA-HQ and AFHQ without using the progressive learning strategy. We show results of image translation using style codes obtained from both style encoder and style generator and report average performance in Table 4. NA means that the model fails in learning and can not generate meaningful results. We can see that the newly added regularization strategies for the descriptor and the translator, i.e.,  $\mathcal{L}_{\text{energy}}$  and  $\mathcal{L}_{\text{mode}}$ , are essential for stabilizing the cooperative training. Especially, the energy-based regularization loss  $\mathcal{L}_{\text{mode}}$  plays an important role to ensure that the translator can quickly catch up with the descriptor toward the



Figure 7: Results for reference generation on AFHQ dataset. The source images (first row) take in the style codes generated by the Style Encoder and reference images (first column) and translates into target domains. We could see the animals’ faces have successfully translated into target domains with consistency in expression.



Figure 8: Qualitative results of cycle consistency check on CelebA-HQ dataset. Each column corresponds to a specific example. The first row displays an image from the source domain A, while the second row shows a reference image from domain B. The third row exhibits the translated image obtained by translating the source image to the target domain specified by the reference image. The fourth row presents the reversed translation results obtained by using the image from the third row and treating the image from the first row as the reference image.

data distribution during the cooperative training because we learn the translator so that its output can minimize the energy function. The  $\mathcal{L}_{energy}$  is useful to obtain performance gain by limiting the magnitude of the energy values. Also, we can find that the performance drops significantly when removing the cycle-consistency loss  $\mathcal{L}_{cycle}$ , which has proved to be a key objective for unpaired cross-domain image translation task.

## 5 Conclusion

We present MD-CoopNets, a novel approach that combines energy-based learning, MCMC sampling, cooperative learning, and progressive learning for unpaired multi-domain image-to-image translation. Our method includes a multi-head energy-based model as a descriptor, capturing the multi-domain image distribution, and a diversified image-to-image translator for cross-domain one-to-many mapping. To train both the descriptor and translator, we introduce a multi-domain MCMC teaching algorithm. Additionally, we propose progressive learning to enhance the scalability and efficiency of our model. Experimental results demonstrate that our approach achieves comparable performance to adversarial learning frameworks and sets a new benchmark in energy-based image-to-image translation methods.





Figure 9: Qualitative results of cycle consistency check on AFHQ dataset. Each column shows one example. The first row displays an image from the source domain A. The second row showcases a reference image from domain B, providing the desired style or specifying the target domain. The third row exhibits the translated image, which is obtained by transforming the source image to the target domain specified by the reference image. The fourth row presents the results of the reversed translation, achieved by utilizing the image from the third row and considering the image from the first row as the reference image.

Table 1: Evaluation on CelebA-HQ dataset.

| Dim | Method       | Reference |      |             | Diverse |       |       |
|-----|--------------|-----------|------|-------------|---------|-------|-------|
|     |              | M→F       | F→M  | Avg         | M→F     | F→M   | Avg   |
| 256 | MUNIT[31]    | -         | -    | 107.1       | -       | -     | 31.4  |
|     | DRIT[32]     | -         | -    | 53.3        | -       | -     | 52.1  |
|     | MSGAN[33]    | -         | -    | 39.6        | -       | -     | 61.4  |
|     | StarGAN2[2]  | 19.8      | 28.0 | 23.8        | 10.0    | 17.6  | 13.8  |
|     | ours         | 19.9      | 30.9 | 25.4        | 22.1    | 32.3  | 27.2  |
| 128 | CycleCoop[8] | -         | -    | -           | 122.4   | 131.9 | 127.1 |
|     | StarGAN2[2]* | 21.1      | 27.2 | 24.2        | 11.9    | 17.6  | 14.8  |
|     | ours         | 14.5      | 22.9 | <b>18.7</b> | 13.7    | 23.0  | 18.4  |
| 64  | CycleCoop[8] | -         | -    | -           | 129.8   | 124.5 | 127.2 |
|     | StarGAN2[2]  | 18.8      | 22.2 | 20.5        | 10.2    | 13.3  | 11.8  |
|     | ours         | 10.8      | 19.3 | <b>15.1</b> | 10.5    | 18.2  | 14.3  |

Table 2: Evaluation on AFHQ dataset for diverse image generation.

| Dim | Method      | D→C  | W→C  | C→D  | W→D  | C→W  | D→W  | Avg  |
|-----|-------------|------|------|------|------|------|------|------|
| 256 | MUNIT[31]   | -    | -    | -    | -    | -    | -    | 41.5 |
|     | DRIT[32]    | -    | -    | -    | -    | -    | -    | 95.6 |
|     | MSGAN[33]   | -    | -    | -    | -    | -    | -    | 61.4 |
|     | StarGAN2[2] | 6.4  | 7.1  | 36.2 | 30.4 | 9.1  | 8.6  | 16.3 |
|     | ours        | 15.8 | 15.4 | 42.5 | 42.4 | 28.4 | 28.5 | 28.8 |
| 128 | StarGAN2*   | 7.1  | 6.6  | 32.9 | 29.6 | 10.2 | 9.4  | 16.0 |
|     | ours        | 12.8 | 13.3 | 36.5 | 35.8 | 11.5 | 11.6 | 20.2 |
| 64  | StarGAN2*   | 8.6  | 7.0  | 34.6 | 28.9 | 15.3 | 17.8 | 18.7 |
|     | ours        | 13.6 | 13.8 | 33.2 | 32.5 | 12.7 | 12.6 | 19.7 |



Table 3: Evaluation on AFHQ dataset for image translation using reference images.

| Dim | Method      | D→C   | W→C   | C→D   | W→D   | C→W   | D→W   | Avg         |
|-----|-------------|-------|-------|-------|-------|-------|-------|-------------|
| 256 | MUNIT[31]   | -     | -     | -     | -     | -     | -     | 223.9       |
|     | DRIT[32]    | -     | -     | -     | -     | -     | -     | 114.8       |
|     | MSGAN[33]   | -     | -     | -     | -     | -     | -     | 69.8        |
|     | StarGAN2[2] | 6.3   | 7.3   | 39.9  | 33.1  | 16.4  | 15.6  | 19.8        |
|     | ours        | 11.2  | 10.7  | 33.1  | 32.8  | 8.5   | 8.2   | <b>17.4</b> |
| 128 | CycleCoop   | 93.5  | 210.4 | 102.8 | 183.8 | 182.2 | 204.2 | 162.8       |
|     | StarGAN2[2] | 7.3   | 9.0   | 37.2  | 33.6  | 8.9   | 10.4  | 17.8        |
|     | ours        | 9.6   | 9.6   | 27.0  | 25.8  | 7.4   | 6.7   | <b>14.3</b> |
| 64  | CycleCoop   | 267.6 | 259.0 | 194.5 | 226.5 | 223.2 | 212.9 | 230.6       |
|     | StarGAN2[2] | 7.3   | 9.1   | 35.3  | 31.0  | 18.6  | 23.6  | 20.8        |
|     | ours        | 11.7  | 10.5  | 24.6  | 24.0  | 7.1   | 7.5   | <b>14.2</b> |



Figure 10: Progressive learning on CelebA-HQ dataset. Translated images are generated by models learned at resolutions of  $64 \times 64$ ,  $128 \times 128$ ,  $256 \times 256$ , respectively. The same source image and reference image are utilized for generating images at each column.



Figure 11: Progressive learning on AFHQ dataset. Translated images are generated by models learned at resolutions of  $64 \times 64$ ,  $128 \times 128$ ,  $256 \times 256$ , respectively. The same source image and reference image are utilized for generating images at each column.

Table 4: Ablation Study on CelebA-HQ and AFHQ datasets in  $64 \times 64$  resolution.

| Removed Item                   | CelebA    |        | AFHQ      |        | Avg   |
|--------------------------------|-----------|--------|-----------|--------|-------|
|                                | Reference | Latent | Reference | Latent |       |
| baseline                       | 15.1      | 14.3   | 14.2      | 19.7   | 17.0  |
| Remove $\mathcal{L}_{diverse}$ | 16.3      | 17.1   | 36.4      | 35.2   | 26.3  |
| Remove $\mathcal{L}_{cycle}$   | 111.0     | 127.3  | NA        | NA     | 119.2 |
| Remove $\mathcal{L}_{energy}$  | 134.5     | 40.7   | 208.5     | 97.6   | 120.3 |
| Remove $\mathcal{L}_{mode}$    | NA        | NA     | 277.2     | 217.6  | 247.4 |

## References

- [1] Yunjey Choi, Min-Je Choi, Munyoung Kim, Jung-Woo Ha, Sunghun Kim, and Jaegul Choo. Stargan: Unified generative adversarial networks for multi-domain image-to-image translation. In *IEEE Conference on Computer Vision and Pattern Recognition (CVPR)*, pages 8789–8797, 2018.
- [2] Yunjey Choi, Youngjung Uh, Jaejun Yoo, and Jung-Woo Ha. Stargan v2: Diverse image synthesis for multiple domains. In *Proceedings of the IEEE/CVF conference on computer vision and pattern recognition*, pages 8188–8197, 2020.
- [3] Jianwen Xie, Yang Lu, Ruiqi Gao, Song-Chun Zhu, and Ying Nian Wu. Cooperative training of descriptor and generator networks. *IEEE transactions on pattern analysis and machine intelligence*, 42(1):27–45, 2018.
- [4] Jianwen Xie, Zilong Zheng, and Ping Li. Learning energy-based model with variational auto-encoder as amortized sampler. In *Thirty-Fifth AAAI Conference on Artificial Intelligence (AAAI)*, pages 10441–10451, 2021.
- [5] Jianwen Xie, Yaxuan Zhu, Jun Li, and Ping Li. A tale of two flows: Cooperative learning of langevin flow and normalizing flow toward energy-based model. In *International Conference on Learning Representations (ICLR)*, 2022.
- [6] Jing Zhang, Jianwen Xie, Zilong Zheng, and Nick Barnes. Energy-based generative cooperative saliency prediction. In *Thirty-Sixth AAAI Conference on Artificial Intelligence (AAAI)*, pages 3280–3290, 2022.
- [7] Jianwen Xie, Zilong Zheng, Xiaolin Fang, Song-Chun Zhu, and Ying Nian Wu. Cooperative training of fast thinking initializer and slow thinking solver for conditional learning. *IEEE Transactions on Pattern Analysis and Machine Intelligence (TPAMI)*, 44(8):3957–3973, 2022.
- [8] Jianwen Xie, Zilong Zheng, Xiaolin Fang, Song-Chun Zhu, and Ying Nian Wu. Learning cycle-consistent cooperative networks via alternating mcmc teaching for unsupervised cross-domain translation. In *Proceedings of the AAAI Conference on Artificial Intelligence*, volume 35, pages 10430–10440, 2021.
- [9] Tero Karras, Timo Aila, Samuli Laine, and Jaakko Lehtinen. Progressive growing of gans for improved quality, stability, and variation. *arXiv preprint arXiv:1710.10196*, 2017.
- [10] Song Chun Zhu, Yingnian Wu, and David Mumford. Filters, random fields and maximum entropy (frame): Towards a unified theory for texture modeling. *International Journal of Computer Vision*, 27:107–126, 1998.
- [11] Yann LeCun, Sumit Chopra, Raia Hadsell, M Ranzato, and Fugie Huang. A tutorial on energy-based learning. *Predicting structured data*, 1(0), 2006.
- [12] Geoffrey E. Hinton. A practical guide to training restricted boltzmann machines. In *Neural Networks: Tricks of the Trade - Second Edition*, pages 599–619. Springer, 2012.
- [13] Jianwen Xie, Yang Lu, Song-Chun Zhu, and Ying Nian Wu. A theory of generative convnet. In Maria-Florina Balcan and Kilian Q. Weinberger, editors, *International Conference on Machine Learning (ICML)*, 2016.
- [14] Erik Nijkamp, Mitch Hill, Song-Chun Zhu, and Ying Nian Wu. Learning non-convergent non-persistent short-run mcmc toward energy-based model. *Advances in Neural Information Processing Systems*, 32, 2019.
- [15] Yilun Du and Igor Mordatch. Implicit generation and generalization in energy-based models. In *Advances in Neural Information Processing Systems 32: Annual Conference on Neural Information Processing Systems (NeurIPS)*, 2019.
- [16] Geoffrey E Hinton. Training products of experts by minimizing contrastive divergence. *Neural computation*, 14(8):1771–1800, 2002.
- [17] Yilun Du, Shuang Li, Joshua B. Tenenbaum, and Igor Mordatch. Improved contrastive divergence training of energy-based models. In *Proceedings of the 38th International Conference on Machine Learning, ICML*, 2021.
- [18] Ruiqi Gao, Yang Song, Ben Poole, Ying Nian Wu, and Diederik P. Kingma. Learning energy-based models by diffusion recovery likelihood. In *The ninth International Conference on Learning Representations, ICLR*, 2021.

- [19] Ruiqi Gao, Erik Nijkamp, Diederik P Kingma, Zhen Xu, Andrew M Dai, and Ying Nian Wu. Flow contrastive estimation of energy-based models. In *Proceedings of the IEEE/CVF Conference on Computer Vision and Pattern Recognition, CVPR*, 2020.
- [20] Taesup Kim and Yoshua Bengio. Deep directed generative models with energy-based probability estimation. *arXiv preprint arXiv:1606.03439*, 2016.
- [21] Tian Han, Erik Nijkamp, Xiaolin Fang, Mitch Hill, Song-Chun Zhu, and Ying Nian Wu. Divergence triangle for joint training of generator model, energy-based model, and inferential model. In *IEEE Conference on Computer Vision and Pattern Recognition (CVPR)*, pages 8670–8679, 2019.
- [22] Rithesh Kumar, Sherjil Ozair, Anirudh Goyal, Aaron Courville, and Yoshua Bengio. Maximum entropy generators for energy-based models. *arXiv preprint arXiv:1901.08508*, 2019.
- [23] Zhisheng Xiao, Karsten Kreis, Jan Kautz, and Arash Vahdat. Vaebm: A symbiosis between variational autoencoders and energy-based models. In *The ninth International Conference on Learning Representations, ICLR*, 2021.
- [24] Will Sussman Grathwohl, Jacob Jin Kelly, Milad Hashemi, Mohammad Norouzi, Kevin Swersky, and David Duvenaud. No MCMC for me: Amortized sampling for fast and stable training of energy-based models. In *The ninth International Conference on Learning Representations, ICLR*, 2021.
- [25] Yang Zhao, Jianwen Xie, and Ping Li. Coopinit: Initializing generative adversarial networks via cooperative learning. *arXiv preprint arXiv:2303.11649*, 2023.
- [26] Jing Zhang, Jianwen Xie, Zilong Zheng, and Nick Barnes. Energy-based generative cooperative saliency prediction. In *Proceedings of the AAAI Conference on Artificial Intelligence*, volume 36, pages 3280–3290, 2022.
- [27] Yang Zhao, Jianwen Xie, and Ping Li. Learning energy-based generative models via coarse-to-fine expanding and sampling. In *The ninth International Conference on Learning Representations, ICLR*, 2021.
- [28] Ruiqi Gao, Yang Lu, Junpei Zhou, Song-Chun Zhu, and Ying Nian Wu. Learning generative convnets via multi-grid modeling and sampling. In *IEEE Conference on Computer Vision and Pattern Recognition (CVPR)*, pages 9155–9164, 2018.
- [29] Martin Heusel, Hubert Ramsauer, Thomas Unterthiner, Bernhard Nessler, and Sepp Hochreiter. Gans trained by a two time-scale update rule converge to a local nash equilibrium. *Advances in neural information processing systems*, 30, 2017.
- [30] Xun Huang and Serge Belongie. Arbitrary style transfer in real-time with adaptive instance normalization. In *Proceedings of the IEEE international conference on computer vision*, pages 1501–1510, 2017.
- [31] Xun Huang, Ming-Yu Liu, Serge Belongie, and Jan Kautz. Multimodal unsupervised image-to-image translation. In *Proceedings of the European conference on computer vision (ECCV)*, pages 172–189, 2018.
- [32] Hsin-Ying Lee, Hung-Yu Tseng, Jia-Bin Huang, Maneesh Singh, and Ming-Hsuan Yang. Diverse image-to-image translation via disentangled representations. In *Proceedings of the European conference on computer vision (ECCV)*, pages 35–51, 2018.
- [33] Qi Mao, Hsin-Ying Lee, Hung-Yu Tseng, Siwei Ma, and Ming-Hsuan Yang. Mode seeking generative adversarial networks for diverse image synthesis. In *Proceedings of the IEEE/CVF conference on computer vision and pattern recognition*, pages 1429–1437, 2019.